Fletcher J. Agostino
Christopher J. Evenhuis
Sergey N. Krylov

Department of Chemistry and Centre for Research on Biomolecular Interactions, York University, Toronto, Ontario, Canada

Received November 1, 2010
Revised December 10, 2010
Accepted December 13, 2010

Research Article

Milli-free flow electrophoresis: I. Fast prototyping of mFFE devices

We coin a term of milli-free flow electrophoresis (mFFE) to describe mid-scale FFE with flow rates intermediate to macro-FFE and micro-FFE (μFFE). Introduced decades ago, mFFE did not find practical applications. We revive mFFE, as we view it as a viable purification complement to continuous synthesis in capillary reactors with product flow rates of ~5 to 2000 μL/min, too small for macro-FFE but too large for μFFE. The development of the tandem of continuous synthesis/purification will require the production and evaluation of a large number of prototypes of mFFE devices. As the first step, we developed a fast (<24 h) and economical (~$10) method for prototyping mFFE devices using a robotic milling machine. mFFE prototypes are constructed from two machined matching poly(methyl methacrylate) (PMMA) substrates, which are bonded in 10 min using dichloromethane to provide a strong and irreversible seal. Using the developed prototyping technology, we designed and evaluated 25 prototypes of mFFE devices. By optimizing the feed rates and rotational speeds of the drills, the depth of the electrode channels, the dimensions of the entrance and exit reservoirs, the sample flow rate, and the diameter and position of the sample input, we were able to achieve indefinitely long operation of the device with cycles of alternating 15-min electrophoresis and 0.5-min regeneration (bubble removal). The test analytes, rhodamine B and fluorescein, were baseline resolved by mFFE for flow rates ranging from 10 to 600 μL/min. These results prove that our prototyping approach is suitable for the challenging task of multi-parameter optimization of mFFE devices.

Keywords: Continuous purification / Fast prototyping / Free-flow electrophoresis / Mechanical milling
DOI 10.1002/jssc.201000758

1 Introduction

Continuous flow microreactors are an attractive means of synthesis. Compared to batch synthesis, they offer: an appreciable increase in product yields through atom economy [1]; reduced costs associated with starting materials; safer operating conditions and better control [2], and the capacity to generate high-throughput production by numbering up [3], in which parallel processing units can be combined to achieve larger scale performance. Progress in this area has been slowed by the lack of a compatible continuous purification technique [4]. In principle, free flow electrophoresis (FFE) would be suitable as a separation technique, but has not yet been implemented due to an incompatibility of scale.

Continuous purification, in FFE, occurs when an electric field causes a separation orthogonal to a continuous hydrodynamic flow of sample and BGE. The lateral separation of components is determined by: differences in their electrophoretic mobilities, the strength of the electric field, and the speed of the hydrodynamic flow. Both macro and microscale FFE (μFFE) devices exist [5–7], but neither is suitable for purification of products from microreactors because the flow rates are too large for μFFE, yet too small for macro-FFE. In 1975, Hannig et al. produced a mid-scale FFE device with dimensions intermediate to macro-FFE and μFFE [8]. The mid-scale alternative was used successfully to separate proteins as well as to evaluate a number of electrophoretic parameters [9]. Typical flow rates used in continuous flow microreactors are within the range of 5–2000 μL/min [2, 10–13]. These flow rates have been optimized to acquire the high yields that microreactors produce. To the best of our knowledge, no method of continuous purification for microreactors has been implemented to date. Here we address this problem, by prototyping a mid-scale FFE device that would be compatible with microreactors; we call this ''milli''-FFE (mFFE). mFFE has the potential to be the first example of continuous purification *in line* with continuous flow microsynthesis.

To fully complement microreactors, it will be necessary to improve the resolution quality typically associated with FFE. Often, components of a reaction mixture have very similar electrophoretic mobilities; thus making their

Correspondence: Professor Sergey N. Krylov, Department of Chemistry, York University, Toronto, Ontario M3J 1P3, Canada
E-mail: skrylov@yorku.ca
Fax: +1-416-736-5936

Abbreviations: **BGE**, background electrolyte; **CH_2Cl_2**, dichloromethane; **FFE**, free flow electrophoresis; **FR**, feed rate; **μFFE**, microscale FFE; **mFFE**, milli-FFE; **PMMA**, poly(methyl methacrylate)

separation very difficult. Non-Orthogonal-to-the-Flow Electrophoresis is a potential solution to improve resolution [14, 15]. To explore any such solution, multiple prototypes will need to be made in a timely and cost-effective fashion.

Modern methods of fabrication include photolithography, hot embossing, and laser ablation; however, they are neither suitable for rapid prototyping, nor are they suitable for fabricating scales larger than μFFE. The first two methods are costly and time consuming to implement and laser ablation is limited by the complexity that can be integrated into potential designs [16, 17]. Using photolithography to fabricate larger scale devices would only incur higher costs, and would be technically impractical for creating millimetre dimensions. Milling machines, however, have the capacity to reproducibly remove material, and to prototype complex geometries rapidly and at low cost. They have been used previously to manufacture microfluidic devices [18–20]. For mFFE, milling is an ideal method for prototyping devices at this scale.

Here, for the first time, we demonstrate the prototyping of an mFFE device using a milling machine. A solution bonding technique was used to irreversibly seal two poly (methyl methacrylate) (PMMA) substrates together in less than 10 min. Combining the fast prototyping capabilities of a milling machine with rapid bonding produced a fully functional device in less than 24 h. Much work was involved to optimize this procedure and to successfully produce a functional mFFE device. This article will concisely inform readers of the optimal parameters needed to reproduce this work. More importantly, with this knowledge prototyping is accelerated and the potential for *in line* continuous purification of microreactor products is significantly enhanced.

2 Materials and methods

2.1 Solid edge

All FFE models were designed using Solid Edge (Siemens PLM, Plano, TX) software. Starting with a 3-D base, features were modeled as 2-D sketches on the surface of the base. The 2-D sketches included a separation channel (60×110 mm), two electrode channels (1.5×110 mm), triangular exit and entrance reservoirs (60×10 mm), circular BGE inlets and outlets (1.8 mm diameter), circular electrode holes (1.8 mm diameter), and circular bubble outlets (3.6 mm diameter). Figure 1 illustrates the setup for this FFE device. These sketches were modified by height or depth by applying a protrusion or cutout function, respectively. The separation channel was 200 μm deep, the electrode channels were 1.15 mm deep, the reservoirs were 0.6 mm deep, and all of the holes were 5 mm deep. These modifications gave the FFE device its defining features. The top and bottom substrates were not identical but had individual features to facilitate bonding between the two faces, and to aid in the proper fitting of the two substrates. The first feature was a protrusion on one side of the face and

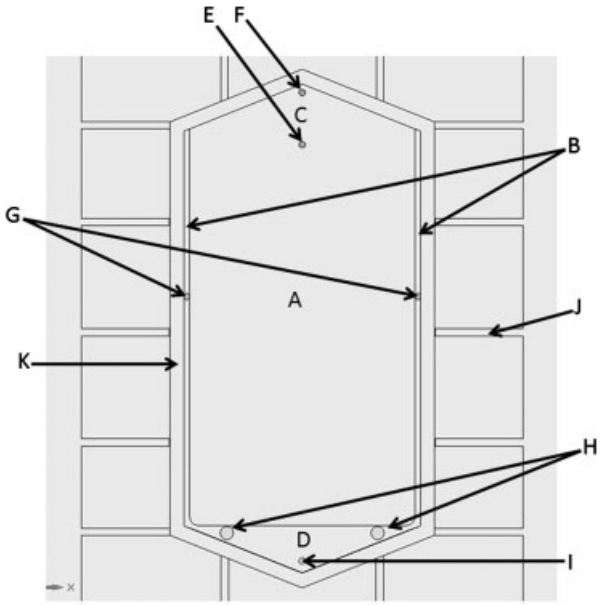

Figure 1. Top substrate of an mFFE device: (A) separation channel, (B) electrode channel, (C) entrance reservoir, (D) exit reservoir, (E) sample inlet, (F) BGE inlet, (G) electrode holes, (H) bubble outlet, (I) BGE outlet, (J) solution bonding channels, and (K) ''snap fit''.

the second was a complementary cutout wherein the protrusion would fit tightly. This relationship was called a ''snap fit''. The cutout of the ''snap fit'' bordered the functional area of the FFE device and was 4 mm wide and 2.5 mm deep. Conversely the protrusion of the ''snap fit'' was 3.75 mm wide and 2.5 mm high.

The third feature was a combination of narrow channels beginning at the edge of the base and touching the edge of the snap fit. These features existed on both faces, and were aligned with each other so that the combined channels were 2 mm wide and 2 mm deep. This depth was chosen so that a long syringe would be able to inject a bonding agent at the snap fit. The fourth feature was two extensions of the device from the base, or wire frames. Their purpose was to act as a support during milling.

2.2 Edge cam and numerical control coding

After Solid Edge designing, the model was exported to Edge Cam (Planit CAD/CAM Software, Tuscaloosa, AL), which is a preparatory software program for milling. In Edge Cam, the piece to be milled was modeled inside a simulated stock material. This stock was created by defining the distance (in mm) between the edges of the stock material and the FFE device. Once the orientation was organized, all defining features were recognized on the model through a ''feature finder'' function. Boundaries were then established to limit milling to specific regions.

The next phase was to prepare milling operations for the features defined within the boundaries. The three

operations that were prepared were: roughing, profiling, and flatlanding. Important parameters were set up to control the milling accuracy: the feed rates (FR); plunge rates (PR); cut increments (CI); and rotational speeds (rpm). The feed rate is the speed at which the tool traverses along the stock material, the plunge rate is the speed at which the tool traverses in a vertical direction, and the cut increment is the depth at which the tool will cut with each successive pass of the drill.

An MDX-540 milling machine (Roland DGA, Irvine, CA) was used to fabricate each device. Roughing removed the bulk material from the stock. The bulk is only removed by verifying the presence of excess stock. By default, Edge Cam assumed that excess stock material has already been removed. If this was not clarified before initiating the operation, the cutting tool would not have recognized its absence and would begin to mill deeper into the stock, potentially damaging the model or the cutting tool itself.

Profiling was the most important operation, as it was responsible for defining the features of the device. Flatlanding was typically a final operation, which created smooth surfaces and removed any remaining stock to achieve the desired depth. Once each milling operation was prepared, numerical control (NC) codes were generated. Numerical control codes are deciphered by the milling machine to execute the operations. PMMA (Johnston Industrial Plastics, Toronto, Canada) was the substrate used to fabricate each FFE device. Table 1 gives a summary of the optimal milling parameters. Each tool (McMaster Carr, Chicago, USA) had its respective role in fabricating the FFE device. Before each operation, the cutting tool was installed into the milling machine and calibrated with respect to its depth. All of the cutting tools were reused. By applying due vigilance, multiple devices were fabricated without breakage. The cost of purchasing the five cutting tools was $200 (CAN). The cost of the PMMA for each device was approximately $10 (CAN). That was the total price of fabrication.

2.3 Order (of tooling) in milling

Each tool had a threshold at which it would break. Using the tools in proper order reduced damage or breakage of the stock material and the tools themselves. Each cutting tool, largest to smallest, performed its milling functions before moving to the next tool. Roughing was always the first operation to be executed. The z-offset was set to a tolerance of 0.3 mm, allowing the 3/8″ cutting tool to remove material to 0.3 mm from the actual surface of the device. The 1/8″ and smaller cutting tools were used for the subsequent profiling operations. In this case no tolerance was programmed so to allow each cutting tool to reach the desired depth.

Flatlanding was performed immediately after profiling with the 1/8″ cutting tool, effectively removing any remaining stock material left behind by the 3/8″ cutting tool, and smoothing the surface. This limited any unnecessary strain on the smaller cutting tools by reducing the depths that these tools need to reach, due to the default assumption that there was no excess material present. If flatlanding was not performed, the smaller tools would mill through this excess material, potentially damaging or breaking the cutting tool.

2.4 Optical transparency and clarity

A UV-Vis spectrophotometer (Beckman Coulter, Oakville, Canada) was used to measure the absorbance of a variety of PMMA pieces flatlanded by the milling machine. The results were compared with a PMMA piece that was not milled.

The clarity of the same PMMA pieces was evaluated visually by observing a coin placed behind each piece. Again, the results were compared with a PMMA piece that was not milled. Both the transparency and clarity experiments were repeated after coating the pieces with mineral oil (Sigma-Aldrich, Oakville, Canada). This was to better represent the optical environment within the mFFE device.

2.5 Solution bonding

All reagents were purchased from Sigma-Aldrich unless otherwise mentioned. Dichloromethane (CH_2Cl_2) was used to bond two pieces of PMMA together. CH_2Cl_2 was

Table 1. Optimal milling parameters

	Operation		
	Roughing	Profiling	Flatlanding
Cutting tool diameter			
3/8″ or ∼9.5 mm	FR: 2000 mm/min PR: 100 mm/min rpm: 3000	N/A	N/A
1/8″ or ∼3.2 mm	N/A	FR: 800 mm/min PR: 100 mm/min rpm: 3000	FR: 200 mm/min PR: 100 mm/min rpm: 3000
1/16″ or ∼1.6 mm	N/A	FR: 650 mm/min PR: 100 mm/min rpm: 4500	N/A
3/64″ or ∼1.2 mm	N/A	FR: 500 mm/min PR: 100 mm/min rpm: 6000	N/A
1/32″ or ∼0.8 mm	N/A	FR: 400 mm/min PR: 100 mm/min rpm: 6000	N/A

N/A (Not applicable) infers that the tool was not used

introduced slowly with a syringe into the specially designed channels and allowed to move along the snap fit. Each subsequent channel was filled with CH_2Cl_2 carefully and allowed to perfuse to the next channel until each channel was filled. The setup was clamped together and allowed to bond for 10 min.

2.6 Resolving fluorescein and rhodamine B

Two solutions were prepared for resolving fluorescein from rhodamine B. The BGE solution consisted of 25 mM 4-(2-hydroxyethyl)-1-piperazineethanesulfonic acid (HEPES) (99.5%) at pH 7. Triton X-100 of 300 μM was added as a detergent. The BGE solution was then filtered with a Millipore Express Plus 0.22 μm filter (Milian, Gahanna, USA). The sample solution consisted of fluorescein and rhodamine B both diluted to 500 μM in the BGE solution.

Polyethylene pipette tips (200 μL) were used as fluidic adapters and polyethylene tubing was used to transfer the solutions from their stock to the FFE device. Loctite® 409 (Henkel, Mississauga, Canada) was used to seal the adapters to the device and allowed to cure for 1 h. Platinum electrodes were installed into the electrode channels and connected with insulated copper wires to a power source. The power source used was a high-voltage Electrophoresis Power Supply EPS 3501 XL (Amersham Pharmacia Biotech, New Jersey, USA). Any openings, holes, or extra spaces were filled with Loctite® to prevent leaks.

The hydrodynamic flow of BGE was driven by gravity. The BGE solution was mounted at a position high enough to force a flow rate of 5–6 mL/min through the chip. The velocity of the sample was measured by observing the position of the sample stream through the separation channel over time. The flow rate of BGE through the separation channel was adjusted to 0.66 ± 0.02 mL/min. This translated to a BGE flow rate of 4.85 ± 0.14 mL/min in the electrode channels. The velocity of the sample stream was driven by a syringe pump (Harvard Apparatus Pump II, Saint-Laurent, Canada) and introduced at a rate of 10 μL/min.

Optical detection was achieved by using a CCD camera (Alphamager, San Francisco, USA). Fluorescence was induced by UV excitation (Alpha Innotech, Santa Clara, USA) and detected through a detector specific to fluorescein. At high concentrations of fluorescein and rhodamine B, a digital camera (Olympus E-10) mounted on a tripod was used to record images.

3 Results and discussion

3.1 Optimization of milling

Tools of all diameters and shapes can be installed in a milling machine to perform the numerous operations that make milling such a versatile and useful method of fabrication. Each operation is unique in that it can reproducibly remove stock material, profile the dimensions into the stock, and flatten the surface to make it smooth. Teamed with this high precision, the milling machine can make incisions that are less than 500 μm in width. Technically, the milling machine also permits depths of as little as 1 μm, but at a risk of its precision. Thus, it is possible to achieve micrometer dimensions in at least one direction.

Preparing an FFE device was achieved in less than 24 h. Figure 2 demonstrates the efficiency of milling machine device fabrication. Solid Edge software is user friendly and contains tutorials for new users to become familiar with designing shaped devices. Modeling FFE designs was a simple task and could be completed within an hour. Adjusting existing designs was intuitive and required only minutes. Calibration and milling preparation were critical to the entire procedure. Placing the PMMA stock in the milling machine was important in order to accurately match the frame of reference designed by Edge Cam. Marking the stock was helpful in attaining accurate orientation.

Fabricating the top and bottom substrates required 11 h to complete. The total time including modeling, calibration, fabrication, bonding, and assembly was 14 h. This time is quoted for an experienced milling machine user; however, for a novice user, the time required should still be under 24 h. Time can be managed more efficiently with instrumental accessories. One such accessory is the automatic cutting tool changer. This would have reduced installation time and also monitoring time.

Caution was exercised when roughing with the 3/8″ cutting tool. The reason for this additional care was to

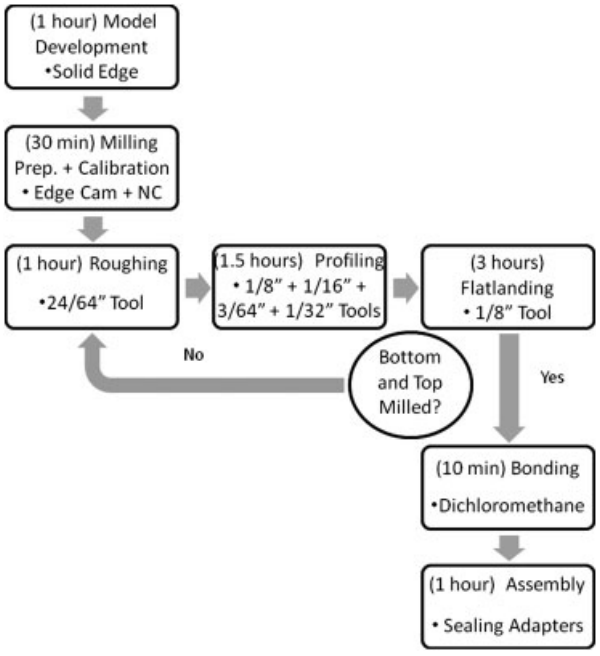

Figure 2. Processes in mFFE device prototyping with a milling machine.

eliminate the adverse effects of excessive force and vibrations associated with this tool. In certain cases, the 3/8″ cutting tool is capable of pushing so strongly in the vertical direction that it could shift the stock downward; this compromises the precision associated with the milling machine. To correct for this issue, support was supplied underneath the stock. Also, reducing the cut increment limited the amount of material through which a tool would drill.

If a procedural error was experienced during milling, it took little time to correct the problem. Milling machines are convenient in that they can re-start an operation at exactly the same place as where they left off. All calibrations are saved and the only setback is to replace the PMMA substrate into the milling machine. Fabrication with the milling machine allowed consistent monitoring, which was a significant benefit for efficient prototyping. Whereas the success of fabricating with other techniques cannot be determined until after fabrication or until after the device has been used.

3.2 Optical transparency and clarity of PMMA

Optimizing the ''milli''-chip itself involved reproducible fabrication of FFE devices that were flat and optically transparent. This was achieved by optimizing the flatlanding operation. The variation of transparency and optical clarity with flatlanding conditions is illustrated in Figs. 3 and 4, respectively. In both figures, panels A–D depict the same milling conditions. In Fig. 3, the optical transparency of A–D is compared. Light scattering is attributed to the substantial increase in absorbance for the pieces that were poorly flatlanded. Using faster FR and rpm, in A and C, resulted in rough and optically obstructed surfaces. At FR = 800 mm/min, the tool does not have sufficient time to properly smooth the surface, and at rpm = 10^4 the tool can potentially melt the surface creating translucence. Melting of PMMA was a significant issue. It not only compromised the optical quality of the surface but melted plastic could accumulate on the surface of the cutting tool making them susceptible to breaking. This was circumvented by decreasing the rpm. Using smaller tools, in A and B, produced the least favorable optical quality as it generated clouded surfaces, a result of melting. The optimal surface clarity, in D, was achieved using the 1/8″ tool, FR = 200 mm/min and rpm = 3×10^3. Similar results are achieved in Fig. 4 when comparing the optical clarity of the pieces. Optical optimization was an important aspect of mFFE prototyping, especially using visual detection.

3.3 Solution bonding

Sealing two PMMA substrates with dichloromethane proved to be an efficient method of bonding, and a rapid means of preparing microfluidic devices. One goal of this work was to develop an efficient means of prototyping devices, and solution bonding proved an exceptional complement to milling. It was solution bonding that allowed prototyping to be accomplished within a 24 h period. There was no significant optimization associated with this technique, as there was for thermal bonding. Thermal bonding is tedious to optimize as it is necessary to find an ideal balance between three variables: pressure, temperature, and time [21, 22]. Without the necessary optimization there is a risk of channel deformation or clogging.

Adhesive bonding works in a similar fashion to solution bonding in that the curing time is comparable. However, one important limitation is that it introduces an increase in height of the separation channel due to the layer of adhesive. For the sake of reproducible microfluidic flows, any additional height is unfavorable and can have adverse effects. Solution bonding was ideal in that CH_2Cl_2 was

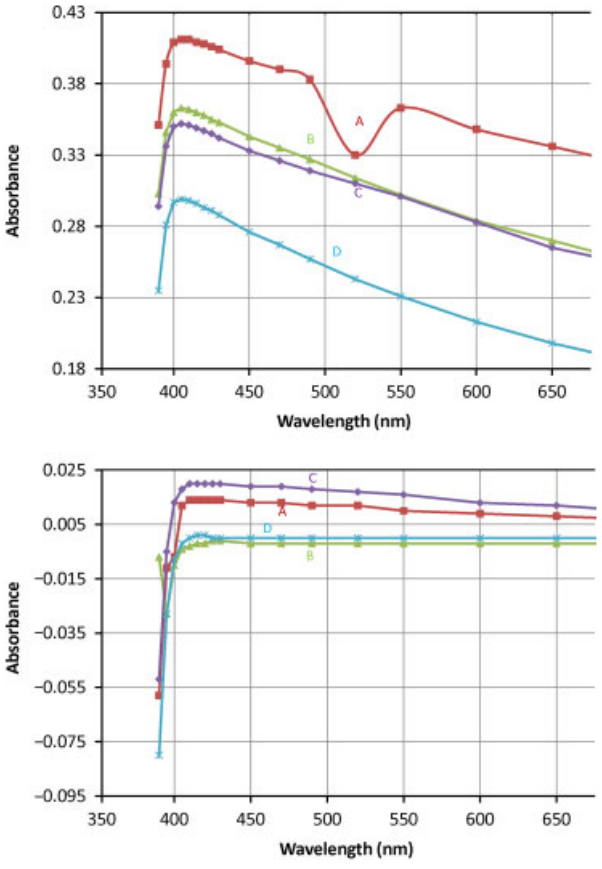

Figure 3. The absorbance of milled PMMA relative to a non-milled piece of PMMA. The differences in measured absorbance reflect the scattering of light. The tool diameters (inches), feed rates (mm/min), and rotational frequencies (revolutions per minute) were used, respectively: (A) ∅ = 1/32, FR = 800, rpm = 10^4; (B) ∅ = 1/32, FR = 150, rpm = 6×10^3; (C) ∅ = 1/8, FR = 800, rpm = 10^4; and (D) ∅ = 1/8, FR = 200, rpm = 3×10^3. The top graph refers to PMMA pieces that were not coated with mineral oil, and the bottom graph refers to PMMA pieces coated with mineral oil.

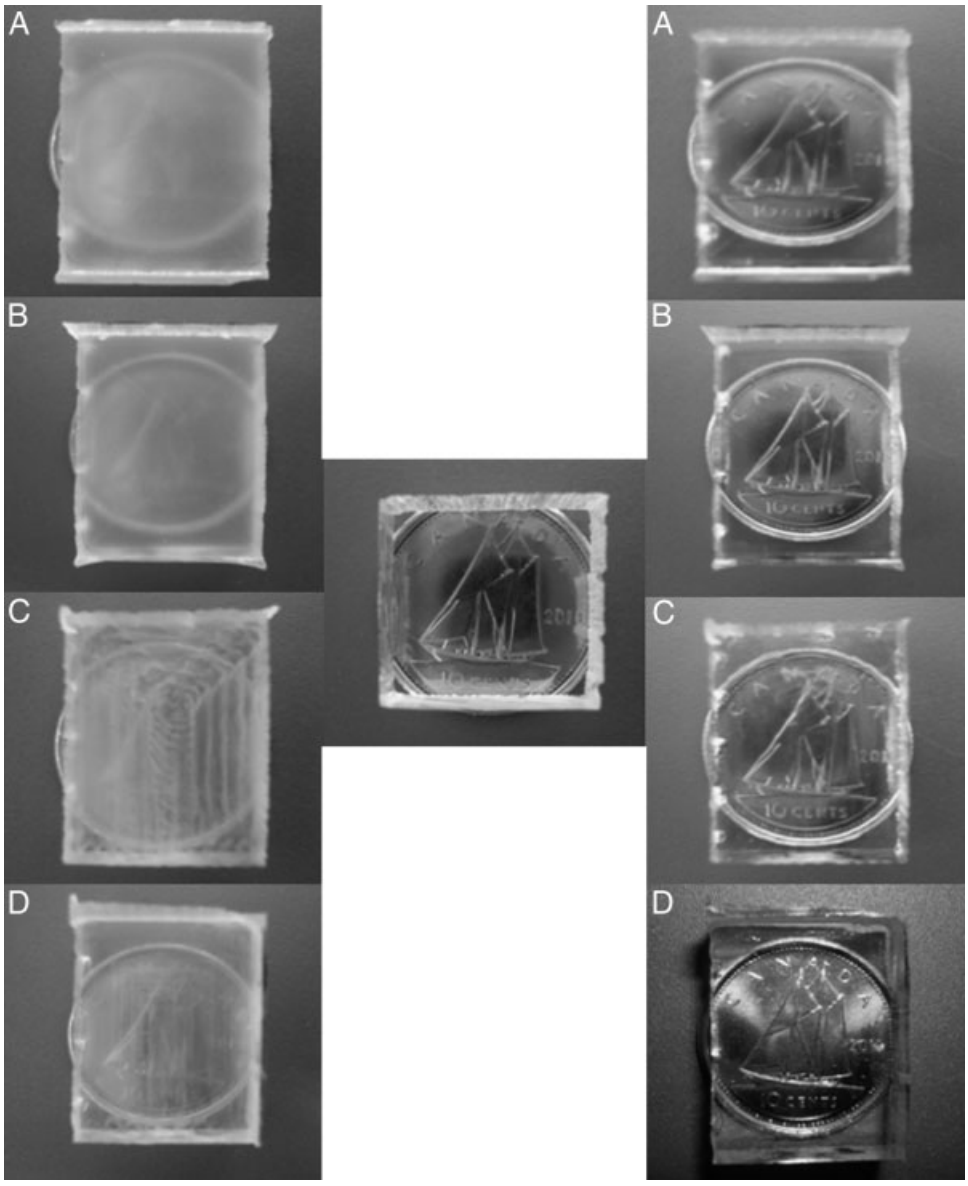

Figure 4. Optical clarity of PMMA. The differences in flatlanding parameters alter the PMMA clarity. At the center is a non-milled piece of PMMA, behind which is a Canadian dime. The panels on the left show the PMMA pieces before coating with mineral oil, and the panels on the right show PMMA pieces coated with mineral oil. The milling conditions compared here are identical to those used in Fig. 3.

added after the device was connected by the snap fits. The channels developed specifically for solution bonding worked perfectly to seal the surfaces together and did not disturb the rest of the device. This was attributed to the orientation of the bonding channels; they were outside of the locations of the ''snap fit'' and separation channel. The ''snap fit'' assembly greatly assisted bonding two pieces together. They work by lining up the two matching pieces perfectly. The use of the bonding channels and ''snap fits'' simplified the bonding process and prototyping overall.

The only risk associated with solution bonding, using dichloromethane, was its possible penetration around the ''snap fits'' causing clogging of the separation channel and/or the loss of optical transparency. This could be circumvented by reducing the volume of dichloromethane used for bonding.

3.4 Improving the quality of separation

3.4.1 Bubble elimination

Of the previously reported methods to limit the effect of bubbles on the electric field strength, the most successful technique was to increase the flow rate within the electrode channels [23]. Once the bubbles were generated, the increased flow rate removed them rapidly preventing them from entering the separation channel and, more importantly, interfering with the electric field. Figure 5 demonstrates by simply increasing the depth of the electrode channels from 1.0 mm, in which the electrode occupied a substantial fraction of the electrode channel, to 1.5 mm, the bubbles generated by electrolysis were effectively prevented from entering the separation channel. Adjusting the height

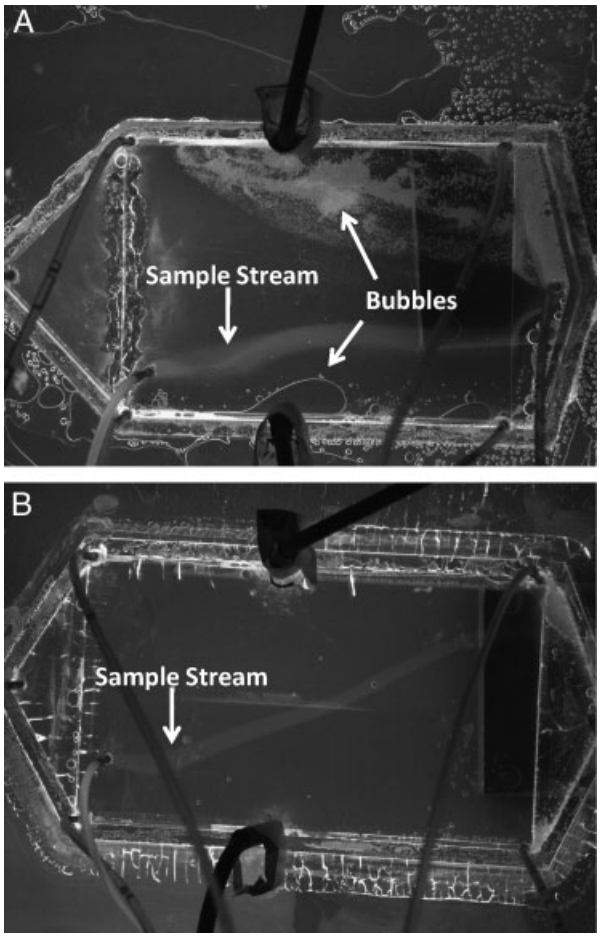

Figure 5. Bubble elimination by increasing channel depth. The sample stream of fluorescein is deflected by an applied voltage of 800 V ($E = 133$ V/cm). The electrode channel depths were (A) 1.00 mm and (B) 1.50 mm. The hydrodynamic flow rate used for both was 0.66 ± 0.02 mL/min.

of the electrode channels was facile using the milling machine. This obviated the need to add membranes to separate the electrodes from the separation channel [24, 25] or the need to add redox additives to the electrode BGEs [26].

3.4.2 Achieving laminar flow

Despite the large size of this FFE device, the 200 μm separation channel depth allowed laminar flow to exist. This was illustrated by calculating the Reynolds number for the flow within the separation channel. A Reynolds number less than 2000 indicates laminar flow.

$$\mathrm{Re} = \frac{\rho v H}{\eta} \quad (1)$$

where Re is the Reynolds number, ρ is the fluid's density, v is the hydrodynamic velocity, η is the viscosity and H is the height of the separation channel. All values for the BGE were approximated to that of water at 20°C.

$$\mathrm{Re} = \frac{(1000\ \mathrm{kg\ m^{-3}})(9.2 \times 10^{-4}\ \mathrm{ms^{-1}})(2 \times 10^{-4}\ \mathrm{m})}{(1.002 \times 10^{-3}\ \mathrm{kg\ m^{-1}\ s^{-1}})} = 0.2$$

The calculated value of Re was well within the laminar realm. The sample entered the separation channel at a point where laminar flow was already established. Diffusional band broadening was limited by the relatively short time spent by the sample in the separation channel.

3.4.3 Ideal positioning and diameter of the sample inlet

Originally, the sample inlet was positioned closer to the electrode channel, and the dimensions of the entrance and exit reservoirs were rectangular. This decreased the control of the sample stream trajectory. The fast flow rate in the electrode channel influenced the direction of the sample; as a result it traversed into the electrode channel in the absence of an electric field. This effect was observed earlier by Fonslow and Bowser, and maintaining linear sample streams was achieved by using triangular entrance and exit reservoirs [27]. Repositioning the sample inlet at the center of the separation channel added versatility with respect to the possible types of separation.

Having already achieved laminar flow, the cause of band broadening was associated with the dimension of the sample inlet. By reducing its diameter from 1.8 to 0.75 mm, the sample stream widths were reduced substantially, thereby improving resolution.

3.4.4 Flow control with a syringe pump

The first resolution experiments were performed using gravity to push the sample into the separation channel. Using gravity, however, resulted in limited control of a consistent flow rate. The sample flow rate was halted upon the application of an electric field, regardless of the electric field strength. The generation of bubbles could be responsible for this effect, because the pressure created by their presence causes a backpressure in the sample capillary. This could be resolved by increasing the height of the sample stock; however, this required precise optimization of the sample height. Unfortunately, the removal of bubbles is not as fast as their generation, thus achieving a consistent sample flow rate was exasperating.

The use of a syringe pump easily rectified this issue, as it precisely supplies a consistent flow rate. The application of an electric field did not adversely affect the sample stream. This allowed resolution to be optimized over a precise range of sample flow rates.

3.4.5 Separation of fluorescein from rhodamine B

A successful separation of fluorescein and rhodamine B was achieved soon after the optimizations of bubble elimination and laminar flow and trajectory (Fig. 6). The two dyes were

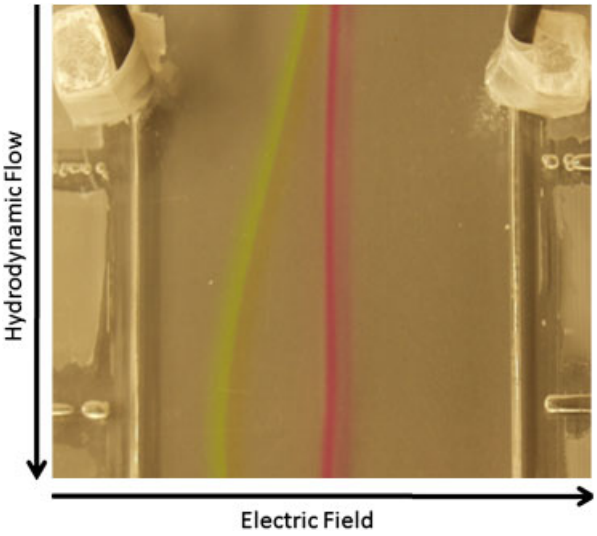

Figure 6. Continuous separation of rhodamine B from fluorescein. A resolution of 9.5 was achieved by applying a separation voltage of 400 V ($E = 67$ V/cm), a resultant current of 6.0 mA; the hydrodynamic flow rate was 0.66 ± 0.02 mL/min, and the sample flow rate was 10 μL/min. The composition of BGE was 25 mM HEPES and 300 μM Triton X-100. The sample concentrations were 500 μM rhodamine B and 500 μM fluorescein. The sample residence time was approximately 80 s. At pH 7.00, fluorescein is negatively charged and migrated toward the anode (+), whereas rhodamine B is neutral and was unaffected by the electric field.

spatially resolved after applying only 400 V (67 V/cm), with a resolution, $R_S = 9.5$. The two streams were narrow and demonstrated little band broadening. The quality of the separation was maintained for at least 15 min without any disruption. After this time, the hydrodynamic flow was increased sufficiently for 30 s to remove the bubbles from the electrode channels, and regenerate the same separation conditions as before. Closer to the exit reservoir, both streams were deflected toward the center. This was a result of having only one outlet. The fluidic profiles were influenced by the positions of both the inlet and outlet. The optimal sample flow rate introduced into the devices was 10 μL/min. This flow rate gave the best resolution and was compatible with the output from continuous flow microreactors.

The scale at which mFFE exists has a number of potential benefits: efficient heat transfer supplied by high surface area to volume ratios; high-throughput capabilities within one device; cost-effective and rapid prototyping platform for microfluidic applications; and most importantly being compatible with microreactors for tandem continuous synthesis/purification.

4 Concluding remarks

FFE continues to develop in both fundamentals and applications [28–32]. Our work will reinforce the area with a tool for fast prototyping of mFFE devices. Below we briefly outline the results. The fabrication and optimization of a fully functional ''milli''-free-flow electrophoresis device using a milling machine have been demonstrated. Fluorescein was resolved from rhodamine B at 400 V (67 V/cm), $R_S = 9.5$. A milling machine was used to manufacture the device in less than 24 h. Solution bonding with CH_2Cl_2 sealed two PMMA substrates in less than 10 min without any leaking or channel deformation. Stable, laminar flow of sample was achieved using a syringe pump. The sample flow rates administered in the ''milli''-chip can be compatible with most continuous flow microreactors. mFFE would serve as a complementary means of continuous purification. As a method of prototyping, milling offers an inexpensive and time-efficient alternative to modern microfabrication techniques based on photolithography, hot embossing or laser ablation, whenever larger devices are involved. By following the protocols described in this article, practitioners will be able to design manufacture and test devices in a much shorter time frame than previously experienced.

Funding for this research was generously provided by NSERC Canada.

The authors have declared no conflict of interest.

5 References

[1] McMullen, J. P., Jensen, K. F., *Annu. Rev. Anal. Chem.* 2010, *3*, 19–42.

[2] Comer, E., Organ, M. G., *J. Am. Chem. Soc.* 2005, *127*, 8160–8167.

[3] Schenk, R., Hessel, V., Hofmann, C., Kiss,J., Löwe, H., Ziogas, A., *Chem. Eng. J.* 2004, *101*, 421–429.

[4] Wiles, C., Watts, P., *Eur. J. Org. Chem.* 2008, 1655–1671.

[5] Hannig, K., Heidrich, H. K., *Free-Flow Electrophoresis*, GIT, Darmstadt 1989.

[6] Roman, M. C., Brown, P. R., *Anal. Chem.* 1994, *66*, 86A–94A.

[7] Křivánková, L., Boček, P., *Electrophoresis* 1998, *19*, 1064–1074.

[8] Hannig,K., Wirth, H., Meyer, B.-H., Zeiller, K., *H.-S. Z. Physiol. Chem.* 1975, *356*, 1209–1223.

[9] Hannig, K., Wirth, H., Schindler, R. K., Spiegel, K., *H.-S. Z. Physiol. Chem.* 1977, *358*, 753–764.

[10] Kockmann, N., Roberge, D. M., *Chem. Eng. Technol.* 2009, *32*, 1682–1694.

[11] Tricotet, T., O'Shea, D., *Chem. Eur. J.* 2010, *16*, 6678–6686.

[12] Rosenfeld, C., Serra, C., Brochon, C., Hadziioannou, G., *Lab Chip* 2008, *8*, 1682–1687.

[13] Baumann, M., Baxendale, I. R., Martin, L. J., Ley, S. V., *Tetrahedron* 2009, *65*, 6611–6625.

[14] Okhonin, V., Evenhuis, C. J., Krylov, S. N., *Anal. Chem.* 2010, *82*, 1183–1185.

[15] Evenhuis, C. J., Okhonin, V., Krylov, S. N., *Anal. Chim. Acta* 2010, *674*, 102–109.

[16] Greener, J., Li, W., Ren, J., Voicu, D., Pakharenko, V., Tangb, T., Kumacheva, E., *Lab Chip* 2010, *10*, 522–524.

[17] Shiu, P. P., Knopf, G. K., Ostojic, M., Nikumb, S., *J. Micromech. Microeng.* 2008, *18*, 025012.

[18] Mei, Q., Xia, Z., Xu, F., Soper, S. A., Fan, Z. H., *Anal. Chem.* 2008, *80*, 6045–6050.

[19] Rodrigues, E. R. G. O., Lapa, R. A. S., *Microchim. Acta* 2009, *166*, 189–195.

[20] Rodrigues, E. R. G. O., Lapa, R. A. S., *Anal. Sci.* 2009, *25*, 443–448.

[21] Sun, Y., Kwok, Y. C., Nguyen, N.-T., *J. Micromech. Microeng.* 2006, *16*, 1681–1688.

[22] Zhu, X., Liu, G., Guo,Y., Tian, Y., *Microsyst. Technol.* 2007, *13*, 403–407.

[23] Fonslow,B. R., Barocas, V. H., Bowser, M. T., *Anal. Chem.* 2006, *78*, 5369–5374.

[24] Raymond, D. E., Manz, A., Widmer, H. M., *Anal. Chem.* 1994, *66*, 2858–2865.

[25] Raymond, D. E., Manz, A., Widmer, H. M., *Anal. Chem.* 1996, *68*, 2515–2522.

[26] Kohlheyer, D., Eijkel, J. C. T., Schlautmann, S., van den Berg, A., Schasfoort, R. B. M., *Anal. Chem.* 2008, *80*, 4111–4118.

[27] Fonslow, B. R., Bowser, M. T., *Anal. Chem.* 2008, *80*, 3182–3189.

[28] Kašička, V., *Electrophoresis* 2009, *30*, S40–S52.

[29] Becker, M., Mansouri, A., Beilein, C., Janasek, D., *Electrophoresis* 2009, *30*, 4206–4212.

[30] Foucher, A. L., Hartmann, K., Hauptmann, M., Wildgruber, R., Safinowski, M., Forst, T., Pfutzner, A., Gelfand, C. A., Nissum, M., *Arch. Physiol. Biochem.* 2009, *115*, 267–278.

[31] Weber, G., Wildgruber, R., in: Schmitt-Kopplin, P. (Ed.), *Capillary Electrophoresis: Methods and Protocols*, Humana Press, Munchen 2008, pp. 703–716.

[32] Turgeon, R., Bowser, M., *Anal. Bioanal. Chem.* 2009, *394*, 187–198.

